831

10/17/90

Expression of Intention to Continue the Study of States Containing Heavy Quarks Using the Wideband Photon Beam and the E687 Multiparticle Spectrometer

Submitted by the Wideband Beam Photon Collaboration

P. Frabetti, Dip. di Fisica dell'Universita' and INFN - Bologna, I-40126 Bologna, Italy

H. Cheung,J. Ginkel,J. Cumalat, University of Colorado, Boulder, CO 80309, USA

J. Butler,I. Gaines,P.H. Garbincius, S. Gourlay,D.J. Harding,P. Kasper, A. Kreymer, Fermilab, Batavia, IL 60510, USA

F. Fabbri, A. Zallo, Laboratori Nazionali di Frascati, I-00044 Frascati, Italy

P. D. Sheldon, J. Wiss, University of Illinois at Urbana-Champaign, Urbana,IL 61801

G. Bellini, M. Di Corato, D. Menasce, E. Meroni, L. Moroni, D. Pedrini,L. Perasso,S. Sala, Dip. di Fisica dell'Universita' and INFN - Milano, I-20133 Milan, Italy

W. Shephard, University of Notre Dame, Notre Dame, IN 46556, USA

S. Ratti,C. Castoldi, Dip. di Fisica dell'Universita' and INFN - Pavia, I-27100 Pavia, Italy

P. Yager, University of California-Davis,Davis,California

A. Lopes, University of Puerto Rico at Mayagues, Puerto Rico

H. Mendes, Cinvestav-IPN, A.P. 14-740,07000 Mexico DF, Mexico

F. Davenport, University of North Carolina at Asheville

J. Filasetta, University of Western Kentucky

J. Wilson, University of South Carolina

APPROVED

Abstract

The spectrometer used in Fermilab Experiment 687 to study the photoproduction and decay of charmed particles will be upgraded to enable it to accumulate 10^6 fully reconstructed charm particles. Capability for detection of B-mesons is also discussed.

The purpose of Fermilab Experiment 687 is to study the production and decay of charm and beauty particles using a high intensity, high energy photon beam, the Fermilab Wideband Photon Beam. The E687 spectrometer is shown in Figure 1. E687 is presently half-way through its second run. In the first running period, from June 1987 to February 1988, a sample of about 10,000 fully reconstructed charm particles was obtained. This sample is now being studied, some examples of the charm signals observed are given in Figure 2. In the first part of the second running period, from February to August 1990, about 5 times more data was collected. It is expected that a similar sample will be collected in the second part of the running period, from December 1990 to the spring of 1991. When the 1991 run is complete, we expect to have a dataset containing 100,000 fully reconstructed charm particles decaying into all charged final states (including those with neutral vees) and a very large sample of states with π^0's, single photons, and η's. These will allow us to explore charm spectroscopy at a level never before achieved and to begin a serious search for bottom photoproduction.

As we look towards the future, there are two natural extensions of the work we have been doing. The first is to continue our studies of charm, which remains a rich subject with many unresolved issues. The second is to try to study bottom photoproduction and decay. In the case of charm, the dynamics of photoproduction is by now well-established and the large samples already in hand allow us to predict with confidence what we can achieve. To address the interesting questions, we will need to obtain a sample of about one million fully reconstructed charm particles, which is one order of magnitude higher than that anticipated in the current run of E687. In the case of bottom, we will not really know whether we have a signal for another year. For the purpose of this expression of interest, we will take as our primary goal the acquisition of a sample of order one million fully reconstructed charm particles. We will, however, note as we go along where the goals of the charm experiment and one more oriented to bottom coincide and where they are in conflict. If it turns out that the full E687 dataset demonstrates an ability to make an important contribution to bottom physics, then we might want to alter the emphasis of the experiment. Fortunately, many of the modifications and upgrades described below for the charm experiment are identical to those required for a bottom-oriented experiment.

This document is organized as follows: Section 1 presents the physics motivation for obtaining a very large sample of charm particles; Section 2 presents one approach to the problem of obtaining the higher photon fluxes required to achieve this goal; Section 3 describes the modifications and upgrades to the spectrometer that are needed to handle the higher intensity (this includes a discussion of changes to the detector, data-acquistion system, and trigger); Section 4 describes additional possible upgrades that will improve the overall efficiency for reconstructing charm and bottom decays and presents a method of achieving even higher beam flux that involves fundamental modifications to the beamline;

Section 5 presents estimates of the computer resources required for offline analysis of this large dataset.

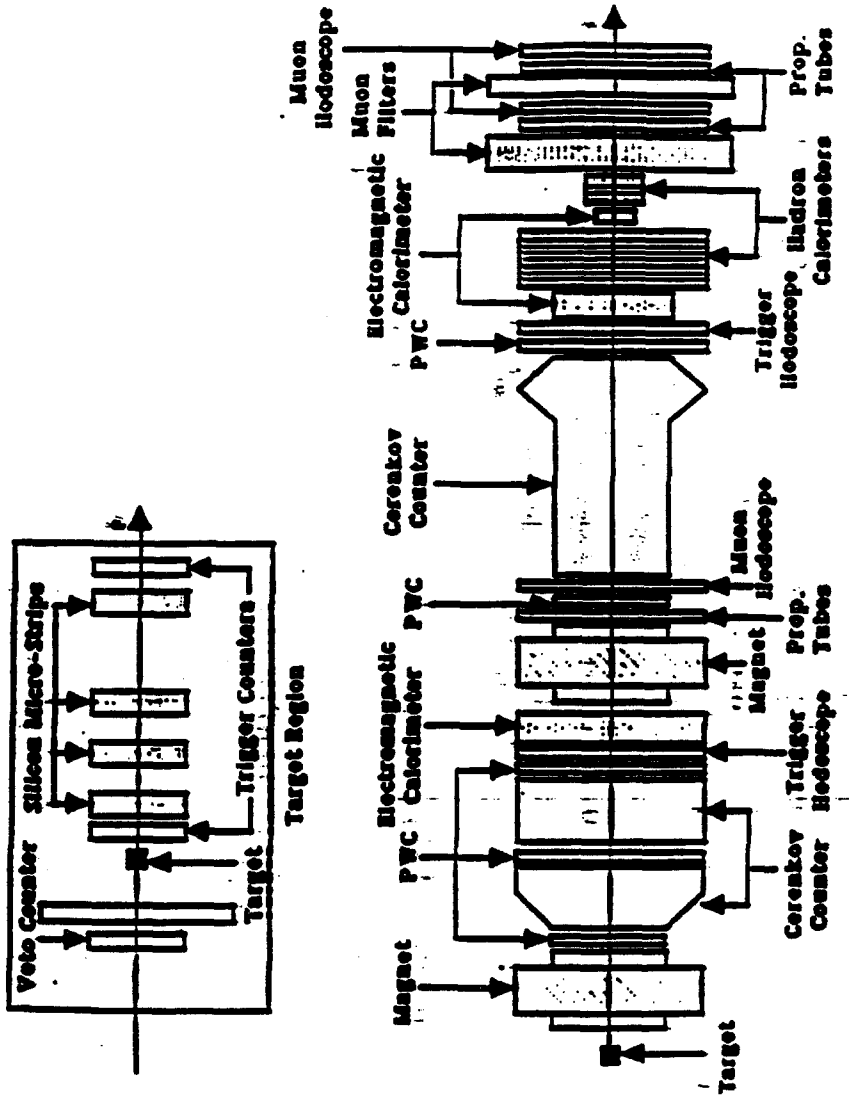

Figure 1: Photon energy spectrum (points, left scale). RESH acceptance (solid line, right scale).

Photon Energy (GeV)

Figure 1: Schematic representation of E687 spectrometer

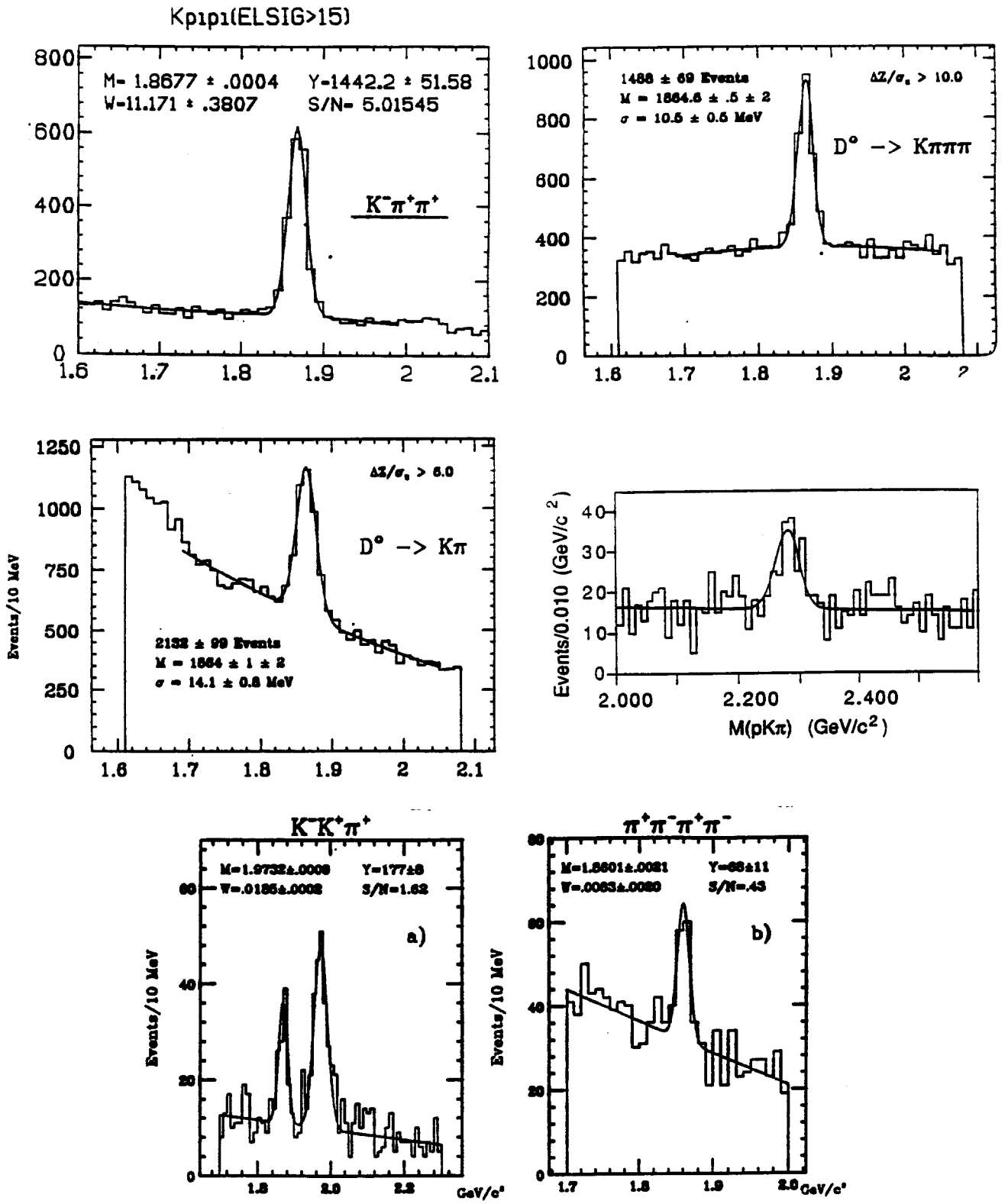

Figure 2: Examples of Charm signals observed in E687

1 Motivation for a High Luminosity Investigation of Heavy Flavors

The subject of charm spectroscopy is now almost 15 years old. However, there are still many areas in which our knowledge is rather limited. Information has been accumulated slowly because of the complexity of the final states, the smallness of the cross sections, the small size of the branching fractions, and the large backgrounds. A major goal of the experiment proposed here is to investigate the open issues in the standard model of charm spectroscopy. For example, this experiment is unique in its ability to study charmed baryons, and should be a major contributor to the study of D^0-$\bar{D}^0$ mixing and semileptonic decays. These and other "programmatic" studies are discussed below. We also list areas where it is possible to search for new physics, beyond the standard model. These searches will emerge as a by-product of the programmatic investigations and will be referred to, following I. Bigi[1], as High Impact Physics studies. Finally, we discuss possible investigations of beauty photoproduction and decay.

1.1 Programmatic Investigations of Charm

1.1.1 D^0-$\bar{D}^0$ Mixing and Doubly-Suppressed Cabibbo Decays

In the Standard Model, the classic mechanism for mixing is the box-diagram. Predictions for D^0-$\bar{D}^0$ mixing are tiny[2], of order 10^{-6}, and would be unobservable by any existing or projected experiment. However, it has been observed that, for the charm quark, the box-diagram that contributes most involves light quarks — s and d. As a result, long distance effects could be important, and final state interactions may have to be taken into account[3]. A recent calculation, which maintains a relatively close contact with existing measurements, predicts a mixing parameter r of 5×10^{-3}[4]. Mixing at this level will be measureable in the proposed experiment. The associated topic of doubly-suppressed Cabibbo decays will also be addressed. These decays should occur at roughly the 0.25×10^{-2} level.

1.1.2 Semileptonic Decays

Semileptonic decays are interesting because they are easier to interpret theoretically than hadronic decays. There are several important measurements to be made. From measurements of semileptonic branching ratios, the proposed experiment could determine the ratio of CKM matrix elements V_{cs}/V_{cd} to 1%. In fact, the measurement of this experiment will be limited by theoretical and systematic errors. The form factors for the D^0, D^+, and the D_s^+ mesons will be determined. An interesting theoretical advance by Isgur and Wise[5] shows that measurements of charm form factors can be used to predict beauty form factors. The polarization of the W in D^0 , D^+ , and D_s^+ decays will be measured, and

interference effects, such as those between the $K^*(890)$ and $K^*(1440)$, will be investigated. Finally, it will be possible to study the semileptonic decays of charm baryons.

1.1.3 f_D – the Pseudoscalar Decay Constant

This parameter is determined by measuring the branching fraction of the decay $D^+ \rightarrow \mu - \nu$. The branching fraction is estimated to be 10^{-4}, hence with 100 million D-decays produced in the experiment, about 10^4 such decays would be on tape. Two methods have been suggested to identify these decays. The first involves using $D^{*+} \rightarrow D^+\pi^0$. The second requires determining the direction of the D^+ by seeing the parent D^+ in the microstrips. Another important fully leptonic decay is $D_s \rightarrow \tau\nu$. This decay can only be reconstructed by observing the parent D_s^+ direction.

1.1.4 D_s^+ and Λ_c^+ Decays

There are many topics to be investigated in the decays of the D_s^+ and the Λ_c^+. This experiment should be able to isolate D_s decays to channels with π^0's and η's and those without a kaon signature. At one time it appeared that there were several missing D_s decay channels. It now appears from work by CLEO and E691 that this is not the case, but several channels need to be measured as this conclusion is based on many assumptions. In addition, it would be extremely valuable to identify decays which proceed only through annihilation diagrams and to examine Cabibbo suppressed D_s decays.

Very little is known about the Λ_c^+. Our group has worked to improve the spectrometer reconstruction capability of Λ's, Σ's and Ξ's. We are planning to add π^0's to some of the channels we presently are investigating. Improved measurements of the relative branching fractions of the Λ_c^+ would aid theorists in providing models of charmed baryon decays.

1.1.5 Meson Spectroscopy

Here the effort would be to study and identify all the D** states and to categorize the states. The D_s^{**} states will also be interesting and will be investigated.

1.1.6 Baryon Spectroscopy and Lifetimes

The observation of charmed baryons requires large statistics and good particle identification. The proposed experiment will be unique in its abilites to study charmed baryon spectroscopy and decay.

At present, very few of the decays of the charm baryon have been measured. Charmed meson decays appear to proceed mostly via two-body decays. From the limited information on charm baryon decays this does not appear to be the case. Scaling from last run where we reconstructed 90 pKπ Λ_c^+ decays, it

Table 1: Predicted yields of charmed baryons

State	Decay	Estimated Events
Λ_c(cud)	p-k-π	9000
Σ_c(cuu)	add π^+	300
Σ_c(cdd)	add π^-	300
Σ_c(cuu)	add π^0	50
Ξ_c(csu)	$\Xi - \pi - \pi$	150
Ξ_c(csd)	$\Xi - \pi^+$	150
Ω_c(css)	$\Omega - \pi$	15

is expected that 9000 Λ_c^+ decays can be obtained from this proposed run and maybe a few hundred p-$\pi - \pi$ and p-K-K events. In the Λ_c^+ to p-K-π decay channel it will be possible to perform a Dalitz plot analysis to investigate two-body versus nonresonant decay mechanisms, to cleanly separate the pK* and $\Delta^{++}K^-$ channels, and to search for possible (and expected) excited p-K Baryon resonances.

Another issue is the relative lifetimes of charmed baryons. The lifetime of the Λ_c^+ is much shorter than the lifetime of charmed mesons. This is presumably due to the fact that the decays proceed principally via the W^+ exchange diagram, since for baryons this diagram is neither helicity nor color suppressed. There are two lifetime predictions[6] that differ on whether the Λ_c^+ lifetime is less than or greater than the Ξ_c and the Ω_c. Estimates for the number of reconstructed events we would obtain for these states are hard to make since our experiment does not yet have clear signals for them. Assuming that the production rate for the Ξ_c (csu and csd) is below the Λ_c by a factor of 10 and down a factor of 100 for Ω_c (css state), our predictions for reconstructed baryon decays are shown in the table 1. The estimate has further assumed that the branching fractions of the Ξ_c to $\Xi^-\pi^+$ and $\Xi^-\pi^+\pi^+$ and of the Ω_c^0 to $\Omega^-\pi^+$ are the same as for the Λ_c^+ to $pK\pi^+$. From the table it seems that the experiment will make a major contribution in addressing baryon lifetime questions.

1.1.7 Charm Photoproduction Dynamics

There are several open issues in charm photoproduction physics. The emphasis of this experiment is to study decay processes and not necessarily production dynamics. It would, however, be very useful to see how pairs of charm particles are produced. For example, how often are baryon-antibaryon pairs produced? Are D_s^+ mesons made with associated D^0 mesons and kaons or are they usually made as D_s - $\bar{D}_s$ pairs? With 1 million reconstructed Charm events, these production dynamics questions will be addressed.

1.2 High Impact Physics

1.2.1 CP Violation

The Standard Model predicts very small levels of CP violation in charm decays. The predicted levels are out of the reach of this experiment or any experiment currently imagined.

It has been pointed out, however, that charm particle decays may be a good place to look for CP violation which is caused by phenomena outside the Standard Model[7]. There are many models which predict levels of CP violation that far exceed the Standard Model predictions. Moreover, there are several characteristics of the charm mesons that make them especially suitable for this kind of search:

- Standard Model CP violation is negligible, so that if CP violation is observed it will be a signal for new physics. In decays of B-mesons, it may turn out that the Standard Model contribution masks any contributions from new physics.
- The charm cross section is large and there are many relatively simple states with high branching fractions that can be used in this kind of exploration.
- The D-decays are self-tagging through the D^*.

CP violation could be observed by looking for a difference between $D^0 \rightarrow \pi^+\pi^-$ and $\bar{D}^0 \rightarrow \pi^+\pi^-$ decays. Similarly, decays to a K^+K^- final state can be used. The parent is found by using $D^{*+} \rightarrow \pi^+ D^0$. E687 presently has about 40 $D^0 \rightarrow K^+K^-$ decays from our 87-88 run. Scaling to this proposed experiment would yield 4000 events. Combined with the decay mode $D^0 \rightarrow \pi^+\pi^-$ the experiment could have more than 5,000 such decays, and would be sensitive to a 2% CP violating asymmetry.

CP violation can also be detected in other ways — for example, by asymmetries of the Vector-Vector decay modes in various angular distributions in D^+ vs D^- decays.

1.2.2 Rare and Forbidden Leptonic Decays

These decays have sensitivity to new kinds of physics. The proposed experiment expects to lower the existing limits by 1 order of magnitude. The decays that would investigated are $D^0 \rightarrow \mu^+\mu^-$, e^+e^-, μ^+e^- and μ^-e^+.

1.3 Possible Investigations of Beauty

The study of beauty physics has been accomplished almost entirely in colliding beam experiments. Argus, CLEO, and now CDF have all contributed to our knowledge of absolute and relative branching fractions of the B mesons.

Presently there is a world-wide quest to observe CP violation in the beauty sector, yet the lifetimes of these particles are still poorly determined. The lifetime measurements are extracted principally through inclusive samples combined with Monte Carlo simulations, which suffer from many assumptions. Only recently has one experiment (Mark II) succeeded in obtaining separate results for charged and neutral B's and the results have large error bars (20%).

In E687 there is the opportunity to contribute to beauty physics using the data set collected in the 1990 run, which is expected to produce 10^5 fully reconstructed charm particles. Certainly the data from the 1990 run should allow us to determine the beauty cross section and enable us to make more accurate calculations for the run proposed here.

With a further factor of ten in statistics, the proposed experiment should fully reconstruct beauty decays and obtain lifetimes for the B^- and the B^0. One of the most important features of the E687 detector is its ability to obtain a direct and clean measurement of beauty lifetimes using the microstrip vertex detector. In the proposed experiment, the observation of beauty should be accomplished through the complete reconstruction of two secondary vertices in cascade. The use of only those tracks associated with the B-decay vertex eliminates the combinatorial background. A precise and separate measurement of the charged and neutral B lifetimes would provide a check of the role of diagrams other than the spectator diagram.

2 Options for Obtaining Higher Flux

We can increase the number of reconstructed charm events by improving the efficiency and acceptance of the spectrometer and by speeding up the data acquisition system (to decrease deadtime). However, the spectrometer already has a rather large acceptance and good efficiency. One can imagine upgrades that will yield a factor of two gain. At least a factor of 5 gain must, therefore, come from increased luminosity. There are several approaches to achieving higher photon intensity. After a brief summary of the beam performance to date, we discuss some of the options.

2.1 Performance of the Wideband Beam

The Wideband beam underwent two upgrades for the 1990-1991 run. The first, the replacement of the beryllium production target by a liquid deuterium target, resulted in an increase in flux by a factor of 1.5, close to the 1.65 that was expected; the second, the use of the positron flux to create photons, resulted in an increase in flux of about 1.45. However, the positron beam had much more "hadronic background" than we expected and was never fully utilized. We investigated this hadronic background from two directions. One effort involved developing a trigger that rejected the hadronic background on the positive side. By the end of the run, the effort had almost produced a successful trigger and offline work has now produced a trigger strategy that will work. The second effort tried to identify and eliminate the hadronic background. It is now rather convincingly established that the background is from Λ decays between the downstream end of the target box sweeping magnets and the first bend in the beam. A large fraction (still being evaluated) can be eliminated by adding a dipole magnet between the downstream end of the target box and the first quadrupole. We believe that with our present understanding we can use the positron beam for real data-taking in the future. The yield in the electron beam at 350 GeV/c is 4.8×10^{-5} electrons per incident 800 Gev/c proton. If the positron beam is used this becomes 7.0×10^{-5} electrons per incident 800 GeV/c proton.

2.2 Options for Increasing the Flux

2.2.1 Change in Incident Beam Energy

If Fermilab is able to upgrade the proton beam energy, the beam flux will increase accordingly. An increase from 800 to 900 GeV/c will result in an improvement of about 1.6.

2.2.2 Change in Secondary Beam Energy

If the primary emphasis of the experiment is charm, then lowering the energy will actually improve the total charm yield. If the energy is lowered to 250 GeV/c the flux increases by a factor of three (and the relative background in the positron beam will drop quite a bit). The overall gain will be about a factor of two due to changes in cross section and acceptance. This option may be exercised if the primary proton energy can not be raised.

2.2.3 Change in Choice of Experiment Parameters

The experimental target can be increased to 15% (from our existing 10%) of an interaction length. In doing this, we lose resolution and acceptance for the interactions in the upstream segments of the target, as the interactions occur further from the microstrip, but do gain in events. We may not gain the entire 50%, but we expect an increase of at least 30%.

It is also possible to increase the radiator. This will increase the number of high energy photons but will also produce dramatically more low energy photons. The ability to do this will depend on how successfully we upgrade the rate capability of the detectors and improve the trigger. It is hard to imagine gaining more than 20-30% by doing this.

2.2.4 Increase in the Number of Incident Protons

We could go from 4×10^{12} to 6×10^{12} protons on target per pulse. This gives us another factor of 1.5. The places where we could have trouble transporting this much beam are in the cryogenic bends and in the LD2 target. The LD2 target is rated at 10^{13} and should be ok. The principal problem is the cryo bends. The bends are supposed to be able to take this rate and we should try a test this year. The bends have taken rates of over 5×10^{12} for short periods of time so there is no reason to believe that this will be a problem. A major question is whether the laboratory would be able to deliver this many protons to us for the duration of the experiment.

2.2.5 Changes in the Production Target

We can increase our acceptance for photons getting thru the 0 degree dump channel to the converter by about 20% by pushing up the deuterium filter so that it is centered where the old beryllium target used to be. This is not easy, as the existing cryostat would have to be modified to fit into the target channel. Another minor improvement would be to put helium into the target box and extend it up to the quadrupoles. Adding helium would decrease the probability for photons to convert to pairs in the target box and after the converter reduce the bremsstrahlung of electrons and positrons. Thus increases the flux by 10%.

Table 2: Summary of luminosity improvements for a charm experiment

	350 GeV	250 GeV	400 GeV
Positrons	1.45	1.45	1.45
LD2 Acceptance	1.2	1.2	1.2
Accelerator Upgrade to 900	1.6	1.3	2.0
Change Energy from 350	1.0	2.0	0.7
More Intensity	1.5	1.5	1.5
Total Gains	4.2	6.8	3.7

2.2.6 Summary of "Conservative" Beam Options

Table 2 gives a summary of what should be viewed as "conservative" approaches to increasing the luminosity. Strategies which require more fundamental changes are described in Section 4. Note that in this table we have not included changes to the experiment's operating conditions, such as more target or more radiator, which were also discussed above and can result in additional increases in the luminosity.

3 Modifications to the apparatus to handle high rates

The main challenge for the apparatus is to be able to handle the increased rate at all levels. Each element will have to operate at at least five times the instantaneous and average rate which it now sees. Because the intensity in the e^+e^- pair region is 500 times that in the rest of the detector, almost all of the difficulties are in the center of the spectrometer. In this section, we discuss how each detector and its associated front-end electronics needs to be modified to handle the increased rates. The required upgrade of the trigger and data acquisition system is also discussed in this section.

3.1 Trigger Counters

To handle an instantaneous rate increase of a factor of 5, our trigger counters will need to be changed. We presently trigger on $\mathrm{TR1 \cdot TR2 \cdot (H \times V)}_{2\ body}$, where TR1 is a single scintillation counter situated between the target and the silicon microstrip, TR2 is a single scintillation counter located immmediately downstream of the microstrip, and H×V is an array of vertical and horizontal counters placed downstream of the last proportional wire chamber, P4. The symbol 2 *body* refers to the fact that we typically require 2 hits in the H×V array. Counters TR1 and TR2 presently operate at 1MHz. At a rate 5 times higher they would barely work.

We have considered two options for replacements of TR1 and TR2. The first option involves replacing these counters with several smaller counters thereby distributing the rate over several phototubes. This choice would obviously work, but since TR1 sets the timing for the entire experiment, then special care would have to be taken when setting up these counters.

The second option would be to replace the scintillators with Cerenkov detectors which are not sensitive to 0 degree pairs. This could , in principle, reduce the trigger rate by a factor of over 100.

The H×V counters would be replaced by triggers from the Hadron Calorimetry. By changing the Hadron Calorimeter from a gas detector to a scintillator readout (see hadron calorimeter section) it will become easy to generate a fast energy sum. Again this would drastically reduce the Master Gate rate. We intend to partially test this idea in the 1991 run by moving part of the H×V array behind the Inner Electromagnetic Calorimeter.

3.2 Microstrip Detector

The microstrip vertex detector is the the E687 spectrometer's most important device for disentangling charm and beauty events from the very large backgrounds. It is installed in the region between the target and the first analysis magnet (M1) and consists of twelve microstrip planes, grouped in four stations

of three detectors each, measuring three coordinates at 135, 45 and 90 degrees with respect to the horizontal axis of the spectrometer.

The innermost central region of the system, covering the very forward production cone, has a resolution two times better than the outer region. The first station,which is the most crucial in determining the extrapolated error to the production point in the target, has twice the position accuracy of the other stations.

Each strip is read out by means of a front-end preamplifier, a remote-end amplifier and a charge integrating FLASH ADC. The analog signal at the amplifier output has a semigaussian shape with a base width of 100-120 ns. In the 1990 run the integration time in the ADC was fixed at 130 ns, giving a signal to noise ratio of about 17 for a single minimum ionizing particle. With a flux of about 10^7 electrons/sec on a 20% Pb radiator and a 10% Be target, about 8% of the events had embedded e^+e^- tracks. These embedded pairs were due either to more than one particle in the same RF bucket or particles from adjacent buckets. The vertex detector sees a pair mainly as a single track at 0 degrees not associated with the production vertex and having a pulse height consistent with 2 minimum ionizing particles.

The overall detection efficiency of every plane is $> 99\%$. The extrapolated transverse error to the mean interaction point in the target (placed 7 cm upstream of the first microstrip plane) is about 9 microns.

The efficiency of the reconstruction code is 96%, on the average, for the tracks of $D\bar{D}$ events, including multiple scattering effects; contamination of spurious tracks is about 2.7%.

In order to face the increased photon flux we plan to replace the front-end preamplifiers of the microstrips with a new design, similar to that used for the beam momentum tagging microstrips, which is being operated at 10 MHz in the present run. The goal is to shorten the gate to 50-60 nsec, thus keeping out-of-time tracks at a reasonable level (pile-up in a single microstrip signal is negligible). Possible further improvements (rotation of the microstrip detectors in the space to have a 0 degrees view in the non bending axis,change of the distance between the target and the microvertex, etc) are under study. We are also considering the possibility of developing a high level trigger for charm events, based on impact parameter.

3.3 Proportional Wire System

The proportional wire system has three planes in each station that are perpendicular (Y) or nearly perpendicular (U,V) to the bend plane. The flux is spread out across many wires. In the non-bend view (X), the entire pair region flux falls on about 10 wires in the center of the chamber. The average rate in the pair region will be about 5 megahz.

There are three different approaches to upgrading the proportional wire system:

- Reduce the need for gas gain by adding preamplifiers to the existing PWC's. This would allow one to lower the voltage by an estimated 300 volts. The mechanical forces would be vastly reduced and the total current pulled from the chambers would be less than they are now.

- Reduce the need for gas gain by reducing the threshold at which the amplifier-discriminators operate. This can be done by separating the chambers, which are packaged 4 per station in a single box, into 4 (or 3) separate boxes. This would decouple the grounds and allow us to run the chambers at about 150-200 volts lower. This has been tested by running with only a single plane instrumented within the existing box.

- Deadening the central region. If this is done, then it is probably desirable to cover this region with some other more robust tracking system.

The plan might vary for the different chamber stations. For the most downstream chamber, P4, the pairs which make it through both magnets are refocussed. This chamber sees the lowest rate from pairs. The pairs would all be concentrated in a $2.5in \times 2.5in$ region except for the effects of bremsstrahlung, which spreads them out vertically. Still, most of the flux is concentrated in a region which is $2.5in \times 10.0in$. The plan would be to deaden this region and to cover it with a small plane with many fewer wires and preamps just downstream of the present plane. P3 has the next lowest rate and we believe that it will be adequate simply to split it into three boxes (X,UV,Y) to reduce the operating voltage. P0, P1, and P2 would probably need at least to be separated into three or four boxes and to have preamps. The hope is to avoid deadening or at worst to just deaden the x-wires. This region would be recovered with some other detector such as very thin wall proportional tubes. Many of these proposed upgrades can be tested with beam in the present configuration and some, such as the threshold reduction, don't need the beam but just require the local electrical environment, mainly the spectometer and beam magnets, to be operating.

3.4 Cerenkov Counters

The Cerenkov system has adequate but not optimal momentum coverage for the future run. The high degree of segmentation in the beam region, coupled with the fact that the beam is reasonably spread out vertically at C1 and C2 allow the counters to survive the high rate environment. If there are problems, they will affect only a few cells in the very center of the counter. The Cerenkov counters are discussed in section 4 in the context of upgrades to improve the efficiency of the detector.

3.5 Electromagnetic calorimeters

3.5.1 Inner electromagnetic calorimeter

The detector is read out in strips. Presently the pairs "paint" a stripe down the middle of the IE. This rate is acceptable at the moment, but as the rate goes up photon reconstruction will be impossible. We will need to block off this region, probably with a vertical stack of lead strips that range out all the electron-positron energy. Presumably this would be a 15 cm thick piece of lead.

3.5.2 Outer electromagnetic calorimeter

This detector is at wide-angle to the beam and should be able to sustain the rate that it will see.

3.6 Muon detectors

The muon proptubes would be replaced with scintillators. The proptubes have a very long gate and would be subject to significant pileup.

3.7 Hadron Calorimeter

The main function of the hadron calorimeter for E687 is to supply a trigger which rejects purely electromagnetic events, mainly e^+e^- pairs, and which enhances the selection of events with charm or beauty quarks. The hadron calorimeter covers only the "inner" detector. In E687 this region is covered by two separate devices: the main hadron calorimeter, which covers the region from 5 milliradians to approximately 30 milliradians, and the "Central Hadron Calorimeter", which covers the central 5 milliradians.

The main hadron calorimeter is an iron-gas sampling calorimeter with tower readout geometry. The absorber consists of 28 iron planes each with dimensions 304cm× 203cm×4.45cm Each plate has a 30cm diameter hole for the beam to pass through. The sum of the plates total 8 proton interaction lengths. The tower geometry allows the formation of a trigger for the transverse energy E_{perp} in addition to a trigger for the total energy E_{tot}. The calorimeter was built to be sensitive to minimum ionising particles for monitoring and calibration purposes.

The severe limitation of this gas calorimeter is that it is slow. The information for the second level trigger is only available at 600 ns after the master gate. For this proposal, the 600 ns delay in making a selection decision is unacceptable. In fact, we propose to put the Hadron Calorimeter into the Master Gate. This choice substantially reduces the Master Gate deadtime and eliminates almost all electromagnetically produced events.

To accomplish these goals we propose to build a conventional hadron calorimeter composed of an iron scintillator sandwich design readout in a strip geometry through adiabatic light guides to large diameter (3 inch) photomultiplier tubes.

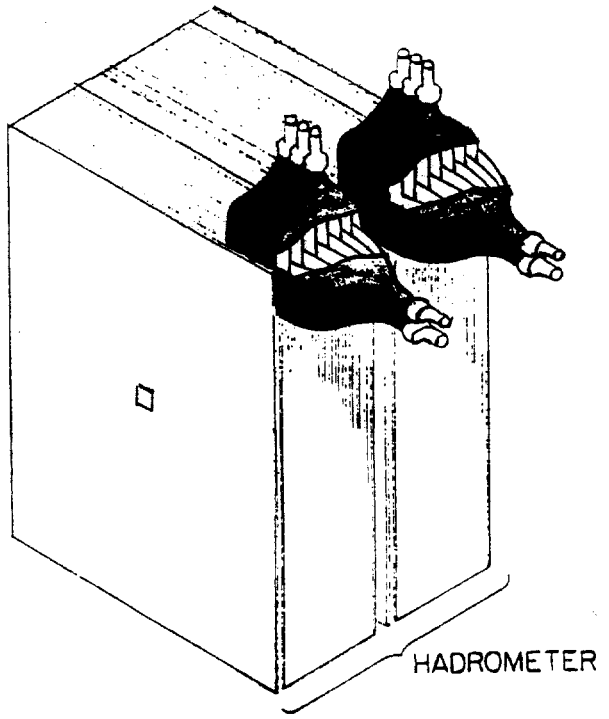

Figure 3: Proposed iron-scintillator hadrometer

We propose to use all the existing cut and machined iron plates, but will reduce the hole in each iron plate from a 30 cm diameter hole to a 16 cm square hole. This involves making 28 iron inserts.

Orthogonal 1 cm thick scintillator strips of vertical and horizontal counters are to be placed in the 28 gaps in the iron. The horizontal and vertical elements are to be located in alternate gaps. Light from the first 7 horizontal strips will be collected into light guides as indicated in Figure 3. Light from the first 7 vertical strips will also be readout into a single photomultiplier tube. The arrangement will be repeated for the downstream 14 gaps. A total of 128 counters will be implemented, with 64 in the upstream section and 64 in the downstream section. The light guides for all 128 counters will be identical. A summary of the needed counters is given in Table 3.

A further drawback of the existing hadron calorimeter is the PAD readout required for the tower geometry. The large pads are responsible for significant noise; hence electromagnetic events in coincidence with this noise can fake a real hadronic interaction. Phototubes and scintillator are very quiet. Contamination from electromagnetic accidentals should be minimal.

Using a scintillator readout allows the total energy and transverse energy sums to be made quickly. The energy sum would be used at the Master gate

Table 3: Proposed Counters for refurbished Hadron Calorimeter

Strip Type	Width (cm)	Length (cm)	Number
Vertical	16	152	48
Vertical - Around hole	16	144	4
Horizontal	16	101	72
Horizontal- Around hole	16	93	4

level. The transverse energy sum would be employed at the second level.

3.8 Beam Instrumentation and Flux Monitors

The current charged particle beam tracking will simply not work. There would be too many instances of two tracks per r-f bucket. We would remove it.

The Recoil Electron calorimetry will probably have severe difficulty with the rates near the undeflected electron beam. The outer counters see much lower rates and will remain useful, primarily for measuring and monitoring the flux and spectrum shape.

The beam gamma shower counter will be replaced by an integrating quantameter which would measure the total electromegnetic energy in the beam. That will provide a normalization and the spectrum shape would be obtained from runs at low intensities.

The Central Hadron Calorimeter will follow the quantameter. The present detector should be able to sustain the additional rate.

3.9 Triggering

The triggering strategy will have to be changed in this experiment. Previously our group has always tried to write out all hadronic events on-line and then sort out the good events in software where more information is available (such as the number of charged tracks in the silicon microstrip). Rates will now be high enough to require that fast decisions need to be made during data-taking.

The e^+e^- pair rate is expected to be 5MHz with a hadronic rate of 5kHz. As explained in the trigger counters section the hadron calorimeter is being incorporated into the Master Gate. It is assumed that all pairs are removed at the Master Gate level. However the hadronic rate is such that we will need to reduce this rate by a factor of 4 before events can be written to tape.

We plan to implement a pulse height trigger on TR1 and TR2 requiring a pulse height equivalent to 3 or more tracks. (If the Cerenkov version of TR1 works, then we will not have an accidental rate problem from pairs.) Further we will require more than 50 GeV of energy deposited in the hadron calorimeter. These two changes are expected to reduce the hadronic rate by a factor of 2.

A final factor of 2 will be gained using an EPERP trigger formed of information from the Inner Electromagnetic Calorimeter and the Hadron Calorimeter.

This trigger is very similiar to the trigger used by E691. In that experiment a factor of 2.5 was gained in the charm to hadron ratio. This EPERP trigger is presently being studied. Studies performed at Breckenridge and at Snowmass indicated that much larger improvement factors could be made if both the inner and the outer spectrometers were used in this trigger.

3.10 Data Acquisition

The problems of triggering and data-acquisition (DAQ) are closely related: the better the trigger, the lower the requirements on the DAQ. We assume that the combination of the first and second level triggers will produce a total of 25,000 events per spill which need to be read in. The average event size is 3 kbytes so the total amount of data is 75 mbytes/spill.

The following is the organization of the present DAQ:

- Front-end digitizing electronics. This consists of special ADC's designed by Milan for the microstrip detector, Lecroy 4290 TDC's, fast latches designed by Fermilab and Lecroy PCOS latches, and Lecroy 1885 ADC's. These are organized into 5 'streams' since the 1885's occupy two FASTBUS crates, each of which is treated as an independent data source. The average readout time for each stream is summarized in table 4.

- "Real-time" data buffering. The data has to be transferred to a buffer as it is read out so the electronics can be freed to record another event. This is presently accomplished using 5 Lecroy 1892 Fastbus 4 mbyte memories, one for each stream. The event fragments are assembled from the 5 memories and sent on to the next level by a 68000 based processor, the GPM, which acts as the FASTBUS master. The average rate which must be handled by this stream is equal to the total amount of data divided by the spill length of about 20 seconds. The data are read through this level quickly to the next level of buffering. This frees the 1892's so they can be used in "circular" mode.

- "Intermediate" buffering. The data are transferred to a larger buffer memory, in this case 10 ACP I nodes with 6 megabytes of memory each. Since these buffers can hold a whole spill's worth of data, writing the data to tape can occur over the spill and the interspill– that is, at an average rate of 1/3 of the rate at which the data is accumulated. The maximum speed of data transfer from these buffers to the data-recording level that has been achieved with the present hardware is 2 mbyte/second.

- Data recording (taping). The data is recorded on up to four 8mm Exabyte tapes in parallel. This allows an aggregate tape-writing speed of 1 mbyte/second.

Table 4: Average readout times for E687 data streams

Data Stream	readout time (μsec)
Microstrips	20
latches	50
TDC's	300-600
ADC (1)	1000
ADC (2)	1000

In order to increase the throughput of the DAQ by a factor of 5 several changes have to be made, although the basic structure and much of the equipment can be preserved. The front-end readout time of 1 millisec/event is obviously not good enough. It needs to be improved to 100 μsec. This would result in a total readout time of 2.5 seconds and a deadtime of only 15%. Obviously, if the trigger rate wound up being a factor of two higher (50,000/spill), the deadtime situation would still be satisfactory.

With 100 μsec average readout time as the goal, table 4 shows that the microstrip stream and the latch stream need no revision. The TDC stream needs to be sped up by a factor of three. We will do this by doubling the number of readout controllers, since it is the data-transfer between the CAMAC crates and the readout controllers that are responsible for most of the time. We also need to use a faster processor in the controllers. The combination of these two improvements should reduce the TDC readout time to below 100 μsec. This leaves the two ADC streams as the major problem.

We know of no good way to upgrade the 1885 ADC's by the required factor of 10. The readout speed is determined by the digitization time of a single 96-channel ADC card plus a readout overhead for each ADC. One could concieve of ways to overlap these times but one is finally limited by the ADC digitization time of 400 μsec.

It will therefore be necessary to change the whole ADC system. There are commercial options available, such as the Lecroy FERA system, which would achieve the required speed. This system is quite expenisive. There is a design for a Fastbus ADC by the Fermilab Physics department which has very fast readout speed and is suitable in all other ways for the experiment and which is estimated to cost less than $75/channel. This would probably be the best choice.

The "real time" buffering is also not adequate to keep up with the higher rates. The solution here is to use the 100 mbyte "Baumbaugh" buffers, originally developed for E687 by Fermilab. The front ends connect easily to these buffers.

The problem of moving the data from the "real time" buffers to the tape can be handled in several ways. Perhaps the most straightforward is to replace the GPM with a fast VME based processor.

The problem of recording the data can be easily handled within the present architecture by simply adding Exabyte tapedrives. Since the present system has more capacity than is currently utilized, doubling the number of drives to 8 is probably adequate and should achieve rates of 2.0 mbyte/sec. These could be upgraded to double density drives if necessary.

In conclusion, the DAQ can be upgraded with existing technology to operate at the required rate. If the trigger rate exceeds the target of 25,000/spill by a factor of two, the "downstream" portion of the system can handle the situation with no trouble. The "front-end" will produce a factor of two more deadtime, which will result in an increase from 15% to 30%, an acceptable situation.

4 Upgrades to Spectrometer to Improve Efficiency

Some part of the improvement in the charm and beauty yield are obtained by improving the efficiency of the spectrometer for reconstructing these events. These improvements are described in this section.

4.1 PWC in the First Magnet

The tracking devices in the E687 spectrometer consist of the silicon microstrip detectors upstream of the first magnet, M1, and the proportional wire chambers, PWC, downstream of M1. While the two systems work extremely well together, there is still a category of wide angle and low momentum tracks which are detected in the microstrip but which don't pass through M1. We could improve our low momentum detection efficiency by installing another wire chamber in the center of M1. Having this chamber in the center of the magnet–halfway between the two systems–would also serve to improve the overall linking efficiency.

This chamber has several advantages and only one disadvantage– that we would have to make it work in a magnet. This chamber would determine the momentum of tracks that don't penetrate all the way through the M1 apperture and would improve our linking efficiency. It would also help to clean up the background from the neutral vees which decay in the magnet. Finally, it would extend the kinematic region over which we are able to identify Σ^-'s, Σ^+'s, Ξ^-'s, and Ω^-'s through their decays to a neutral daughter and a charged track.

4.2 Pixel Detectors in the Target Region

Pixel detectors have only been used in experiment NA-32 at CERN, however experimenters are now discussing using these devices in other experiments and in the SSC detector designs. The two dimensional position information allows for an additional requirement that a track pass thru the predicted point. By having a Pixel Detector upstream of a supposed secondary vertex, one can require that no track in the secondary vertex originate from the primary vertex. One can also,in the case of a charged parent, require that the parent pass thru the predicted pixel.

It would be possible to place a pixel detector directly downstream of the Beryllium target. The device would cover an area 3×3 cm^2 with an array of 500×500 pixels. This device would significantly clean up our signals and should allow access to signals that are otherwise unattainable.

Our group has not done much work on pixel devices, but we are following the advances in the field. Improvements in these detectors, especially in the readout speed, would be necessary before such a device could be used at the rates expected in this experiment. Should a new group join that wishes to finance and build such a device we would encourage the effort.

Table 5: Characteristics of the Čerenkov Counters

Counter	Gas	Threshold (GeV/c)			No. of Cells
		Pion	Kaon	Proton	
C1	HeN_2	8.4	29.6	56.4	90
C2	N_2O	4.5	16.2	30.9	110
C3	He	17.0	61.0	116.2	100

4.3 Cerenkov Counters

This section reviews the layout and performance of the present E687 Cerenkov system, and discusses possible improvements for a new run. Our basic conclusion is that the existing system performs well for much of the charm and beauty physics of a new photoproduction run but several improvements could significantly extend the capabilities of the experiment – particularly in the areas of electron identification for semileptonic decay physics.

The present E687 Cerenkov system consists of three multicell Cerenkov counters with different Cerenkov thresholds. Table 5 summarizes the cell count and thresholds for the existing Cerenkov system.

Low momentum (or wide angle) tracks which fail to traverse the M2 aperture are analysed by both C1 and C2; tracks which traverse the M2 aperture are analyzed by all three counters. The existing Cerenkov system allows protons and kaons to be separated from pions over a momentum range of 4.5 GeV to to 61 GeV and provides unambiguous electron identification for momenta up to 17 GeV for tracks traversing the M2 aperture. We used pure helium in C3 in order to achieve the highest possible Cerenkov threshold available using an atmospheric pressure counter. The Cerenkov thresholds of C1 and C2 were matched to the C3 threshold to provide a continuous momentum range for particle identification (e.g. the kaon threshold of C1 matches the proton threshold of C2 and the proton threshold of C1 matches the kaon threshold of C3).

The present E687 Cerenkov counter system performed well in both the 1988 and 1990 run period. Figure 4 shows an inclusive, combined $D \rightarrow K\pi, K2\pi$,and $K3\pi$ signal obtained in our 1988 run with and without Cerenkov identification requirements on the kaon. About 60% of the total charm signal survives the Cerenkov cut. If one considers cases where the kaon traverses the M2 aperture and thus has a chance of being identified by C3, the kaon is Cerenkov identified as definite kaon or kaon/proton ambiguous about 70 % of the time. These identification fractions include the effects of Cerenkov confusion due to overlapping tracks as well as the effects of the finite Cerenkov identification momentum range. The good performance of the present Cerenkov system can also

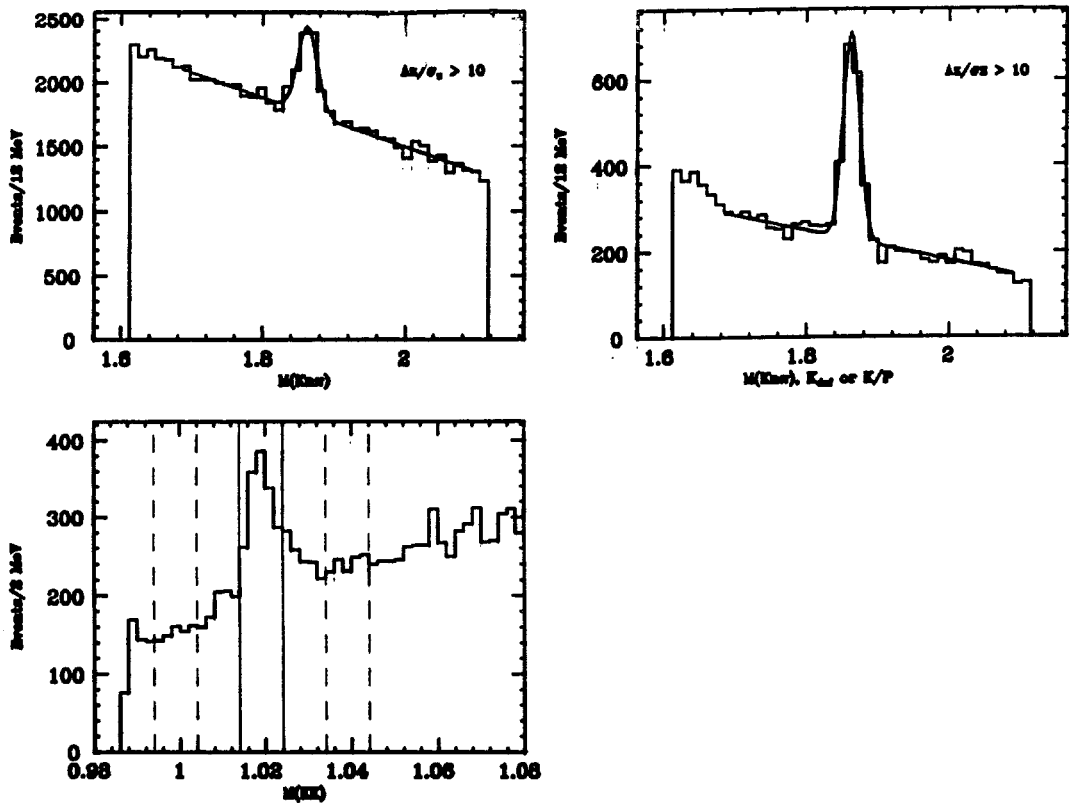

Figure 4: Performance of Cerenkov counters

be confirmed through the decays $\phi \rightarrow K^+K^-$, $K_s \rightarrow \pi^+\pi^-$ and $\Lambda \rightarrow P\pi^-$. Roughly 80% of protons from Λ decays are identified as proton or kaon/proton ambiguous in our 1988 data.

The kaon identification range of the Cerenkov system performs well for many of the charm and beauty physics goals of E687. Figure 5 shows a simulation of the kaon spectrum for otherwise accepted photoproduced $D \rightarrow K\pi$ candidates created by running the wide band beam at an endpoint energy of 350 GeV. Figure 6 shows the integral of this kaon momentum spectrum and shows that about 18 % of kaons have momentum exceeding 61 GeV which is the kaon identification momentum limit of the present Cerenkov system. Although the bulk of kaons from charm decay can be identified with the present system, the finite particle identification range does create a significant inefficiency for charm particles at large x_f. The upper curve of Figure 7 shows the geometrical acceptance for $D \rightarrow K^-\pi^+\pi^+$ decay in the E687 apparatus as a function of x_f. The lower curve shows the geometrical as well as particle identification acceptance for the present Cerenkov system. The high x_f region is important for some tests of the photon-gluon fusion (PGF) model. In particular the PGF model predicts an increased forward-backward peaking of the charm quarks with respect to the incident photon direction with increasing photon gluon center of

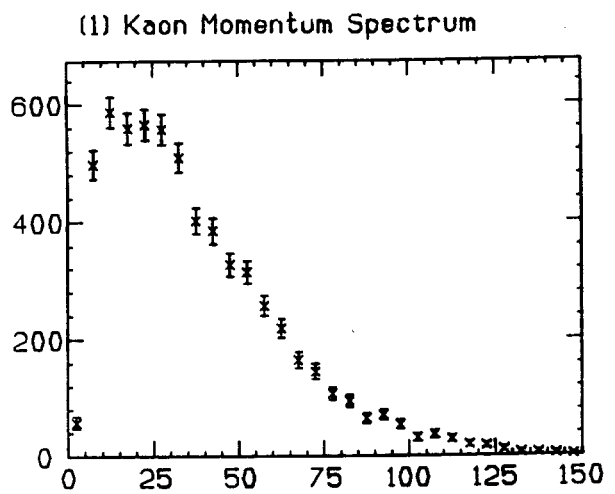

Figure 5: Kaon momentum spectrum

mass energy. The most sensitive tests of this effect require reasonable acceptance at high x_f.

Precision study of charm semileptonic decay is expected to be an important goal of a future high statistics photoproduction run. Electron identification has proven to be crucial for our charm semileptonic decay analysis. Electrons are identified in E687 using our excellent electromagnetic calorimetry in conjunction with Cerenkov identification. The identification provided by the Cerenkov system is essentially complementary to that provided by electromagnetic calorimetry. Comparison of the electron's magnetically deduced momentum to its calorimetrically deduced energy is most effective at high momenta. The present Cerenkov system provides an independent handle on electron identification for electrons below the C3 threshold of 17 GeV where calorimetric identification is more difficult. Figure 8 shows the electron spectrum obtained in a simulation of photoproduced $D^+ \rightarrow K^* e\nu$ decays. Although a reasonable fraction of semileptonic secondaries are in a momentum region amenable to Cerenkov identification, it would certainly be desirable to increase the identifiable momentum range beyond 17 GeV in order to further complement calorimetric electron identification.

One can easily contemplate two types of upgrades of the present E687 Cerenkov system – (1) improving the performance of the present threshold Cerenkov counters, and (2) increasing the range of Cerenkov identification by building a RICH (Ring Imaging CHerenkov counter). At present, both C2 and

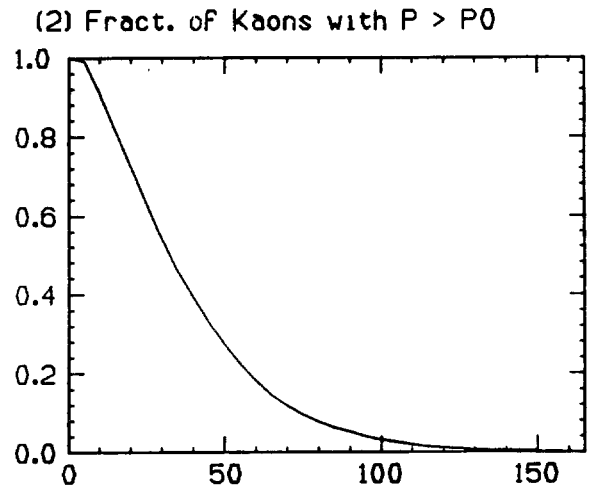

Figure 6: Integrated kaon spectrum

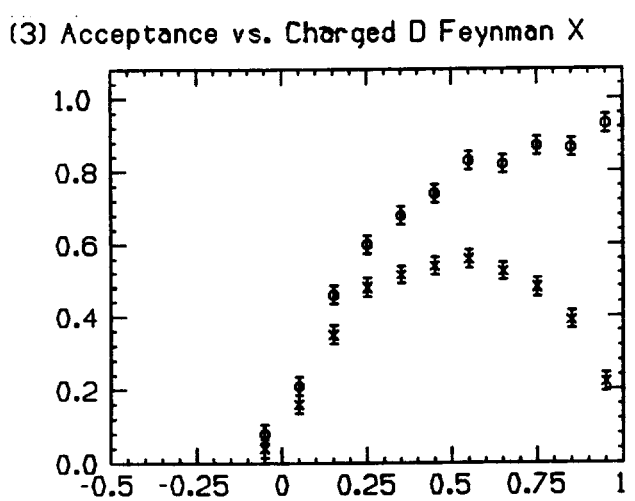

Figure 7: D acceptance vs x_f with and without Cerenkov requirement

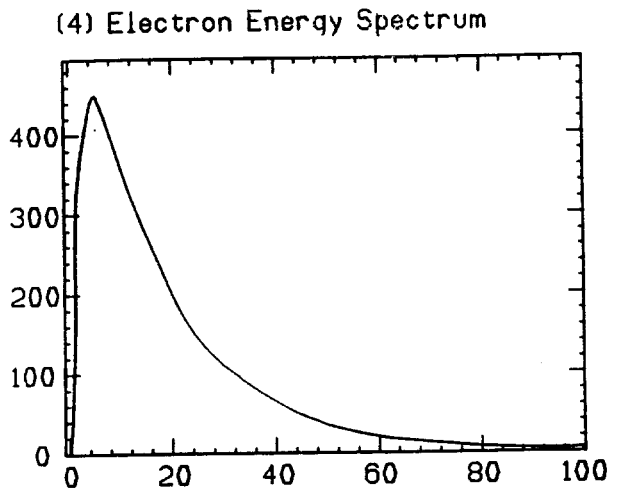

Figure 8: Electron spectrum from semi-leptonic D decays

C3 have close to optimal performance with asymptotic photoelectron yields in excess of 8 photoelectrons. The photoelectron yield of C1 is about 3 photoelectrons primarily owing to its small physical length (only about 1.4 meters) and relatively high pion threshold (8.4 GeV). It would be relatively easy to extend the C1 radiator length. A 2 foot extension would raise the photoelectron yield to about 4.3 photoelectrons. Extra photoelectrons would significantly solidify particle identification for the case of well isolated tracks and decrease the level of Cerenkov confusion for the case of tracks which partially overlap the same Cerenkov cells. The penalty of a 2 foot extension would be a 12 % increase in the P0 $\rightarrow$ P2 lever arm, which, however, has a negligible effect on the total acceptance.

A more radical Cerenkov upgrade involves the incorporation of a Ring Imaging Cerenkov counter which would significantly increase the momentum range for both electron and kaon Cerenkov identification. The original design of the E687 Cerenkov system had a provision for a Ring imaging Cerenkov read out for the central section of C1 designed to extend the momentum range. Figure 9 shows the mirror that would be employed. The original Cerenkov design called for Cerenkov light striking the central 33 cm by 33 cm section of C1 to be imaged by a 1.5 meter focal length mirror on to a two dimensional photon position detector (constructed out of a multi-anode microchannel plane) with $\sigma = 200$ micron position resolution. The RICH section of C1 would subtend ± 25 milliradians which is matched to the solid angle of the M2 aperture. A RICH provides

an independent mass measurement for the track for each measurement of the Cerenkov ring radius. A device with 200 micron spacial resolution and a 1.5 meter focal length mirror offers 2σ kaon - pion mass separation up to momenta of 150 GeV *for each detected photoelectron.* A 2σ electron-pion separation (per photoelectron) would exist up to momenta of about 45 GeV. Time ran out in the development of this device for the 1988 run but the room still exists for a C1 RICH section for a future run.

4.4 Fundamental Change in the Style of the Beam

Another possibility of increasing our photon yield is to go to a 0 degree beamline and use a deuterium or,if gutsy, a tritium filter. Clearly this beam would produce the highest intensity and energy possible in a photon beam. The photon energy would be as high as 800 GeV. The beam has the interesting advantage that there is no infrared catastrophe as in a bremsstrahlung beam. Low energy photons are Compton scattered out of the acceptance. The pair rate from this beam run at the same intensity as the double band would be roughly 1/10 the number of pairs of the double band. Finally this beam would have no problems with synchrotron radiation since there are no bends. To take advantage of these gains we would need to move the target box toward our experiment. Presently the target box is 1200 feet away from our experiment. We would want it more like 500 feet away. The rates, energy reach, and lower pair rate are the advantages. The disadvantages are the hadronic contamination from K_L^0 and neutrons, the closer proximity of the target box to the experiment– i.e. more muons, and the loss of transporting a beam of electrons and pions into our hall for calibration beams. Finally, it would be very expensive to move our target box. An alternative is to examine the possibility of producing the beam from our existing target box. We obviously lose by a factor of (500 feet/1200 feet)**2 and probably a little more. If we assume that we want a beam at our experimental target of 3cm x 3cm, then we have an acceptance of 9 nanosteradians. The actual photon yield at this position was calculated by Jim Wiss at the summer Snowmass meeting. This beam is similar to the old E87 beam. Scaling from that experiment we have roughly 1 photon to 1 neutron to 1/12 K_L^0 at the production target. After a filter– say 10 neutron interaction lengths– we have only gone thru 3.4 pair creation lengths and 6.6 K_L^0 interaction lengths. Thus the ratio of particles after the filter is 1 photon to 1/820 neutrons to 1/400 K_L^0. These numbers are shown in Table 6. This uses 10 interaction lengths of deuterium. Table 7 shows the same numbers for 10 interaction lengths of tritium.

In examining the numbers from these tables it is observed that the photon beam is roughly 3 times more clean if we use tritium as opposed to deuterium. The photon beam is roughly 3 times more intense. So you might argue that tritium is 10 times better than deuterium.

Finally, another possibility is to keep all our options open. We could remove the existing neutral dump and replace it with a deuterium filter. The idea of

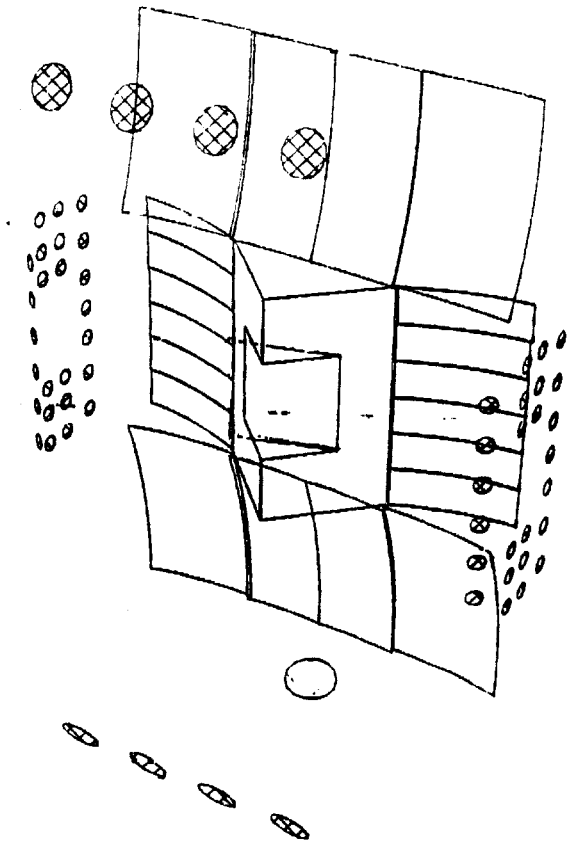

Figure 9: Mirror for RICH

Table 6: Neutral beam with Deuterium filter

Particle	At production	After Filter	Interactions at our target
Photons	1	1	1
Neutrons	1	1/820	1/2.5
K_L^0	1/20	1/600	1/3.0

Table 7: Neutral beam with Tritium filter

Particle	At production	After Filter	Interactions at our target
Photons	1	1	1
Neutrons	1	1/2200	1/6.72
K_L^0	1/20	1/1560	1/8.06

this "triple" beam is to use the high energy photons from the filter and add to the intensity from the double band beams. A final comment on the 0 degree beam is that if we learned to remove hadrons from the beam, then the photon flux could increase still another factor of 10.

5 Computing Requirements

The data-analysis for the present run of E687 is extrapolated to require 400 VAX/780-years for the first pass reconstruction. Since the data-set anticipated for the 1993-1994 run is 5 times larger, it is reasonable to estimate a requirement of 3000 VAX/780-years. We use a factor of 7.5 rather than 5 because the trigger will preferentially eliminate the lowest multiplicity, simplest events. We anticipate reducing computer use by approximately a factor of two by not performing the whole analysis on every event. One possible strategy would be to perform all the track reconstruction and fast particle identification algorithms (< 40% of the present offline analysis package) and only further analyze those events with evidence for a secondary vertex, or unusual final state particles (e.g. multiple kaons and protons and/or leptons). From our present analysis, we estimate that less than 20% of the events will survive these selection criteria. (We have previously skimmed with an algorithm that selected 10% of the events while still being 80% efficient for reconstructable charm decays.) Extensive hadron and electromagnetic calorimetry would only be performed for the skimmed events. This should result in a requirement of 1500 Vax years. If one takes the point of view that 1100 additional VAX/780-years will need to be acquired for this experiment, then, assuming $100/VUP by 1993, the incremental cost of the computing is $110,000. It should be noted that the proposed gains come from doing less analysis on events which are already believed to be uninteresting, not by doing a less-than-complete microstrip or spectrometer tracking. We will, of course, investigate whether partial tracking can further reduce the CPU requirement.

References

[1] I. Bigi,$D^0\bar{D}^0$ Mixing and CP Violation in D Decays- Can There Be High Impact Physics in Charm Decays?, Tau-Charm Factory Workshop,SLAC,Stanford,May,1989

[2] A. Datta and D. Kumbhakar,Z.Phys.C,27(1985),515

[3] Lincoln Wolfenstein,Phys. Lett.,164B,(1985)170

[4] P. Colangelo,G. Nardulli, and N. Paver, Phys. Lett. B, 242(1990)71

[5] N. Isgur and M. B. Wise, Weak Decays of Heavy Mesons in the Static Quark Approximation,Phys. Lett,232B,113,1989

[6] M.B. Voloshin and M.A. Shifman, ZH. Eksp. Teor.Fiz. **91**,1180 (1986) and B. Guberina ,*et.al.*,Z.Phys **C33**,297 (1983)

[7] I.I. Bigi "CP Violation in D Decays", p169-195, Tau-charm Factory Workshop,SLAC,Stanford, May 23-27,1989
and Ling-Lie Chau "CP Noninvariance: A Charm Possibility" p695-705, Tau-charm Factory Workshop,SLAC,Stanford, May 23-27,1989